J Solid State Eletrochem (2004) 8: 482–487
DOI 10.1007/s10008-003-0468-7

ORIGINAL PAPER

Y. K. Zhou · B. L. He · F. B. Zhang · H. L. Li

Hydrous manganese oxide/carbon nanotube composite electrodes for electrochemical capacitors

Received: 28 June 2003 / Accepted: 29 September 2003 / Published online: 9 January 2004

Abstract A novel type of composite electrode based on hydrous manganese oxide and a single-walled carbon nanotube has been prepared and used in electrochemical capacitors. Cyclic voltammetry, galvanostatic charging/discharging tests and electrochemical impedance measurements were applied to investigate the performance of the composite electrodes with different ratios of hydrous manganese oxide and single-walled carbon nanotube. For comparison, the performance of pure hydrous manganese oxide and pure carbon nanotubes was also studied. In this way, the composite electrode with a 6:4 ratio of hydrous manganese oxide to carbon nanotube was found to be the most promising active material for an electrochemical capacitor, which shows both good capacitance and power characteristics.

Keywords Carbon nanotube · Composite electrode · Electrochemical capacitor · Hydrous manganese oxide

Introduction

Electrochemical (EC) capacitors have attracted much attention owing to their high power capability and long cycle life. The EC capacitor can be used for power enhancement and cycle life improvement of primary power sources such as batteries and fuel cells. It has been demonstrated that the hybrid power source, which places the EC capacitor and battery side-by-side, can significantly improve the pulse power performance of batteries [1, 2, 3, 4]. The possible applications for hybrid power sources include space communications, digital cellular phones, and electric and hybrid vehicles. In order to achieve maximum performance in such applications, EC capacitors with high power and energy densities are critical [4, 5].

The amorphous hydrous ruthenium oxide (α-$RuO_2{\cdot}nH_2O$) is known as the most promising material for high power and energy density EC capacitors because of its high specific capacitance and excellent cyclability [6]. However, the high cost of the material itself and the environmental unfriendliness of electrolytes such as acidic media lessen its commercial attraction. Recently, amorphous manganese oxide (α-$MnO_2{\cdot}nH_2O$) has received attention as a new candidate for solving these problems [7, 8].

As α-$MnO_2{\cdot}nH_2O$ shows high resistivity and the equivalent series resistance (ESR) of α-$MnO_2{\cdot}nH_2O$ electrode is very large, carbon should be added as a conducting agent to increase the electrical conductivity [9]. It is well known that carbon nanotubes have obvious advantages over active carbon, for example, low resistivity, high stability, a highly accessibly surface area and a narrow distribution of pore sizes [10]. Hence, in this work, we added carbon nanotubes to α-$MnO_2{\cdot}nH_2O$ to form α-$MnO_2{\cdot}nH_2O$/carbon nanotube composite electrodes to observe their performance. In addition, the performance of a pure carbon nanotube electrode and the role of the carbon nanotubes in the composite electrode are discussed.

Experimental

α-$MnO_2{\cdot}nH_2O$ was synthesized by oxidation of aqueous $MnSO_4$ with $KMnO_4$ solution at pH≈10.6, as described previously by Shan et al. [11]. Carbon nanotubes were prepared and purified as described by Li et al. [12]. TEM and HRTEM were conducted at 200 kV using a JEM-2010 (JEOL) instrument.

The composite electrode materials were made by mixing α-$MnO_2{\cdot}nH_2O$ and carbon nanotubes in a ball mill. The mixing ratio of α-$MnO_2{\cdot}nH_2O$ to carbon nanotubes was 8:2, 6:4, 4:6 and 2:8. For comparison, pure α-$MnO_2{\cdot}nH_2O$ and carbon nanotubes were also used as active materials. In addition, composite electrodes composed of α-$MnO_2{\cdot}nH_2O$ and graphite with different weight

Y. K. Zhou · B. L. He · F. B. Zhang · H. L. Li (✉)
College of Chemistry and Chemical Engineering,
Lanzhou University, 730000 Lanzhou,
People's Republic of China
E-mail: lihl@lzu.edu.cn
Tel.: +86-931-8912517
Fax: +86-931-8912582

fractions (8:2, 6:4, 4:6 and 2:8, respectively) were also prepared as comparison.

The electrode was formed by mixing 80 wt% active material, 15 wt% acetylene black and 5 wt% PTFE as binder before rolling into a thin sheet of uniform thickness. Pellets cut out of the sheet were pressed with a hand oil press onto a Ni-foam current collector (1×1 cm^2).

The electrode performance was measured in a beaker-type electrochemical cell equipped with the working electrode, a platinum counter electrode and a standard calomel reference electrode (SCE). The electrolyte was a 0.5 M Na_2SO_4 aqueous solution and the geometric surface area of the working electrode was 1 cm^2. Cyclic voltammetry scans were recorded from −0.2 to 0.8 V at a scan rate of 5 mV/s using a CHI660A electrochemical workstation (Covarda). Charge/discharge cycle tests were performed using a LAND Celltest (Wuhan, China) at different constant current densities, with a cutoff voltage of −0.2 to 0.8 V. Impedance measurements were performed on a CHI660A electrochemical workstation (Covarda) in the frequency range from 100,000 to 0.01 Hz, and the a.c. modulation was controlled at 5 mV.

Results and discussion

A TEM image of the carbon nanotubes used here is shown in Fig. 1. From it the abundant rope-like nanotube networks are observed, and the support material and other contaminants could hardly be found in the sample. Shown in the inset is a typical high-magnification TEM image, from which high-quality individual single-walled nanotubes with a diameter of around 1.3 nm is clearly observed.

Figure 2 shows the cyclic voltammograms (CVs) of different composite electrodes between −0.2 and 0.8 V versus SCE, taken at a sweep rate of 5 mV/s. Curves a, b, c, d, e and f correspond to pure carbon nanotubes, 8:2, 6:4, 4:6, 2:8 composite electrodes and pure α-$MnO_2{\cdot}nH_2O$, respectively. All these curves show no peaks, which indicates that the electrode capacitor is charged and discharged at a constant rate over the complete cycle. Moreover, these CVs show a mirror image with respect to the zero-current line and a rapid current response on voltage reversal at each end potential, namely, the rectangular-like and symmetric *I–E* responses of ideal capacitive behavior are clearly observed. Figure 2 shows, under such conditions, that the carbon nanotube electrode has minimal specific discharge and charge capacitances, and the specific capacitance increases as the α-$MnO_2{\cdot}nH_2O$ content increases. This is because the carbon nanotubes have only electric double layer capacitance, while a larger faradaic pseudocapacitance occurs for α-$MnO_2{\cdot}nH_2O$. The composite electrode d shows the largest specific capacitance, which is even higher than that of f and e. This may due to the added carbon nanotubes reducing the electronic resistivity of the electrode and increasing the overall electrode porosity. With the help of the added carbon nanotubes, the accessible specific capacitance increases as the available active material increases and therefore the specific capacitance increases rapidly. The composite d shows the appropriate ratio of α-$MnO_2{\cdot}nH_2O$ to carbon nanotubes for which the specific capacitance reaches the maximum. However, accurate capacitance values should be obtained from the constant charge/discharge tests.

Figure 3 shows the constant current charge/discharge curves for different working electrodes. The cutoff voltages for charging/discharging were −0.2 and 0.8 V with a 5 mA/cm^2 current density. For all these curves, a good linear variation of potential versus time was observed, which is another typical characteristic of ideal capacitor behavior. The measured specific discharge capacitance values for a, b, c, d, e and f are 38.0, 65.0, 116.1, 160.7, 141.5 and 127.2 F/g, respectively. The

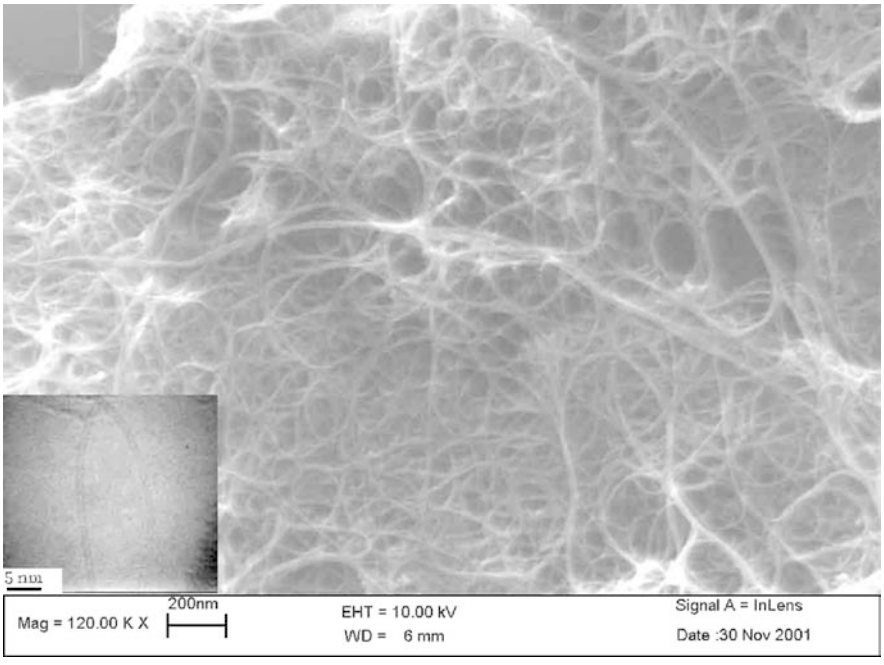

Fig. 1 TEM image of carbon nanotubes (shown in the *inset* is a typical HRTEM image)

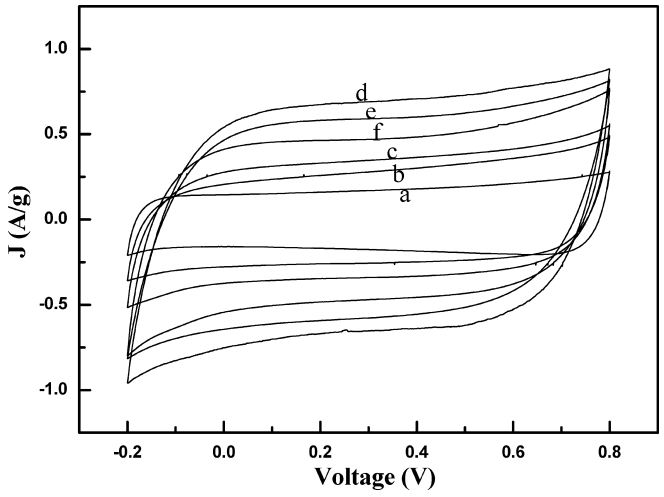

Fig. 2 Cyclic voltammograms of different composite electrodes and pure electrodes. Curves *a–f* represent pure carbon nanotubes, 8:2, 6:4, 4:6 and 2:8 composite electrodes and pure α-$MnO_2{\cdot}nH_2O$, respectively. Scan rate: 5 mV/s

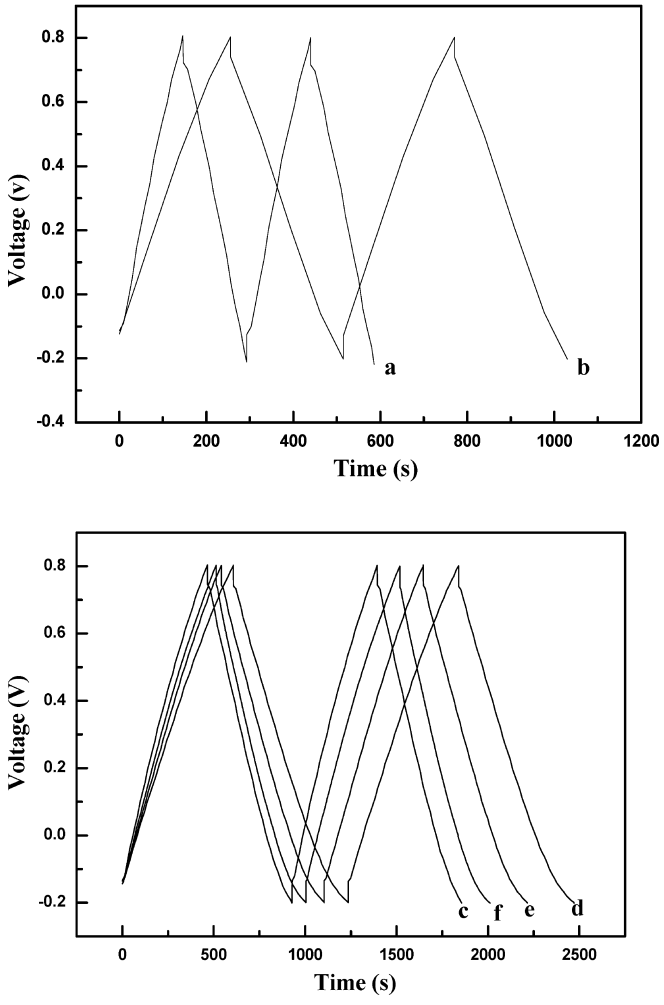

Fig. 3 Galvanostatic charge/discharge curves for different composite electrodes and pure electrodes. Curves *a–f* represent pure carbon nanotubes, 8:2, 6:4, 4:6 and 2:8 composite electrodes and pure α-$MnO_2{\cdot}nH_2O$, respectively. Current density: 5 mA/cm^2

carbon nanotubes initially have a minimal capacitance value of 38.0 F/g; then, as faradaic pseudocapacitance occurs, the capacitance increase as the α-$MnO_2{\cdot}nH_2O$ content increases. Interestingly, the composite electrode d shows the largest capacitance, higher than the pure α-$MnO_2{\cdot}nH_2O$ and the others. Here the result is agreement with that of the CV tests, and the role of the added carbon nanotubes is proved.

To investigate the performance of the composite electrode, all of these electrodes were charged/discharged at different current densities. Figure 4 shows the specific capacitance as a function of charge/discharge current density for all these electrodes. The special capacitance was obtained from Eq. 1:

$$C = \frac{I\Delta t}{\Delta V} \tag{1}$$

The pure carbon nanotubes show almost unchanged specific capacitance of about 40 F/g when the current density is altered. This is because the carbon nanotubes exhibit almost only electric double layer capacitance, and have low resistivity and a highly accessible surface area; also the polarization is very small and the reversibility of the electrode is very good when the current density increases. The contrary case is f, the pure α-$MnO_2{\cdot}nH_2O$ electrode. This shows the largest specific capacitance, 385.4 F/g when the current density is 1 mA/cm^2, but as the current density increases the specific capacitance decreases rapidly, owing to the high resistivity and the strong polarization of this electrode. For the other composite electrodes, as the α-$MnO_2{\cdot}n$-H_2O content alters, the specific capacitance decreases to some extent as the current density increases. The composite electrode d shows a larger specific capacitance even when the current density is bigger. This indicates that d has the best performance with the proper ratio of carbon nanotubes to α-$MnO_2{\cdot}nH_2O$.

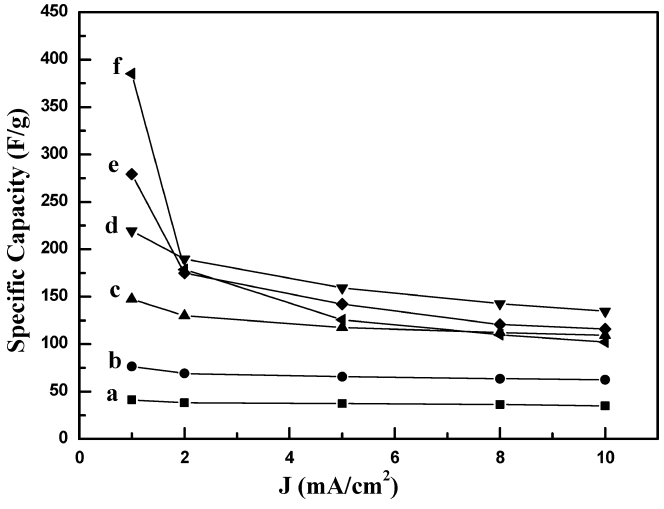

Fig. 4 Specific capacitances of different composite electrodes and pure electrodes as a function of current density. Curves *a–f* represent pure carbon nanotubes, 8:2, 6:4, 4:6 and 2:8 composite electrodes and pure α-$MnO_2{\cdot}nH_2O$, respectively

The power characteristics of different kinds of composite electrodes and pure electrodes were also investigated. Figure 5 shows the normalized capacitance of different electrode materials. Normalized capacitance was obtained using Eq. 2:

$$\text{Normalized capacitance} = \frac{C}{C\ (1\ \text{mA/cm}^2)} \quad (2)$$

The carbon nanotubes showed the best power characteristics between 1 mA/cm^2 and 10 mA/cm^2 current density, while the α-$MnO_2{\cdot}nH_2O$ showed the worst. From Fig. 3 it is shown that the specific power can be improved by adding carbon nanotubes to α-$MnO_2{\cdot}nH_2O$ to form a composite electrode. To investigate the effect of the additive type, α-$MnO_2{\cdot}nH_2O$/graphite composite electrodes were also prepared and tested. The specific capacitance values of different kinds of α-$MnO_2{\cdot}nH_2O$/carbon nanotube and α-$MnO_2{\cdot}nH_2O$/graphite composites are summarized in Table 1. The specific capacitances for the α-$MnO_2{\cdot}nH_2O$/carbon nanotube composite electrodes are consistently higher than those of the corresponding ones with the same weight fraction of additive. The results especially show that α-$MnO_2{\cdot}nH_2O$/carbon nanotube composites containing lower amounts of α-$MnO_2{\cdot}nH_2O$ exceed the performance of α-$MnO_2{\cdot}nH_2O$/graphite composites with larger amounts, i.e. the specific capacitance of the former with a ratio of 4:6 is higher than the latter with 8:2. This means that the active sites of α-$MnO_2{\cdot}nH_2O$ may be increased with less carbon nanotube than graphite and therefore the specific capacitance is greatly increased. At higher rates, this point becomes more obvious. It implies that the electronically conducting network and the nature of the contact between the conductive component and the MnO_2 phase may be an important consideration for achieving higher specific capability; from this point of view, carbon nanotubes are much superior to graphite for use as a conductive component. In fact, the carbon nanotubes have a particular hollow tube structure with low resistivity and highly accessible surface area compared to graphite, the proper addition of which may enormously improve the contact between the α-$MnO_2{\cdot}nH_2O$ particles, and the surface of the α-$MnO_2{\cdot}nH_2O$ particles far from the current collector can work as an active site for a faradiac reaction rapidly and therefore a better performance may be obtained.

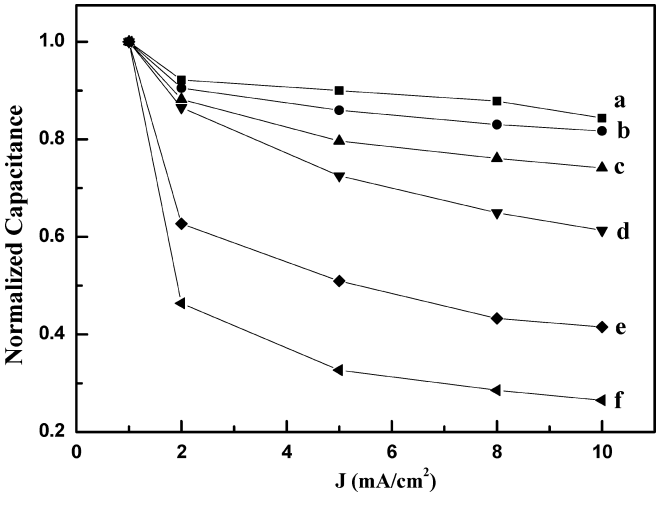

Fig. 5 Comparison of capacitance decays for different electrodes as a function of the discharge current density. Curves *a–f* represent pure carbon nanotubes, 8:2, 6:4, 4:6 and 2:8 composite electrodes and pure α-$MnO_2{\cdot}nH_2O$, respectively

Electrochemical impedance spectroscopy, as a powerful technique for the investigation of the capacitive behavior of electrochemical cells, has been also used to check the ability of the composite materials to store electrical energy. Figure 6 presents Nyquist plots of the composite electrodes and pure electrodes. All the impedance spectroscopy is almost similar in form, composed of one semicircle followed by a linear part at the low-frequency end. At very high frequencies, the measured resistance is composed of the following terms: the ionic resistance of electrolyte, the intrinsic resistance of the active material, and the contact resistance at the active material/current collector interface. We can see that although the intrinsic resistance of the material is different, the very high frequency resistance is roughly the same, about 2.2 Ω. At high frequencies, Fig. 6 shows the presence of a semicircle, which has been described as a pseudo-charge transfer resistance and is associated with the porous structure of the electrode [13]. The semicircles a and b are almost the same, and c and d only increase a little; however, for e and f, there is a rapid increase. For double layer charging only, semicircles in the high-frequency range of the impedance of porous electrodes were also discussed by the presence of occluded pores [14]. Here we can see that carbon nanotubes and the carbon nanotube composite electrodes contain smaller occluded pores in the electrode and therefore smaller pseudo-charge transfer resistance; when the α-$MnO_2{\cdot}nH_2O$ content further increases, the occluded pore amount and pseudo-charge transfer resistance increase rapidly. This may due to the added carbon nanotubes having a low resistance; also it may change the porous structure of the electrode and facilitate the charge transfer.

Table 1 The specific capacitance values (F/g) for different kinds of α-$MnO_2{\cdot}nH_2O$/carbon nanotube and α-$MnO_2{\cdot}nH_2O$/graphite composites

Current density (mA/cm^2)	1	2	5	8	10
Pure MnO_2	385.46	178.56	127.28	109.98	102.06
MnO_2–SWNT (8:2)	279.18	174.96	141.59	120.78	115.92
MnO_2–SWNT (6:4)	219.57	189.89	160.76	142.60	134.63
MnO_2–SWNT (4:6)	147.42	130.01	116.15	112.19	109.31
MnO_2–SWNT (2:8)	76.39	69.13	65.07	63.43	62.43
Pure SWNT	41.45	38.16	37.62	36.36	34.92
MnO_2–graphite (8:2)	100.72	90.45	79.25	68.76	64.55
MnO_2–graphite (6:4)	97.57	73.28	60.36	51.52	49.55
MnO_2–graphite (4:6)	80.63	55.78	49.51	41.72	40.49
MnO_2–graphite (2:8)	49.42	40.36	34.91	31.26	29.45
Pure graphite	1.59	1.25	1.24	1.2	0.68

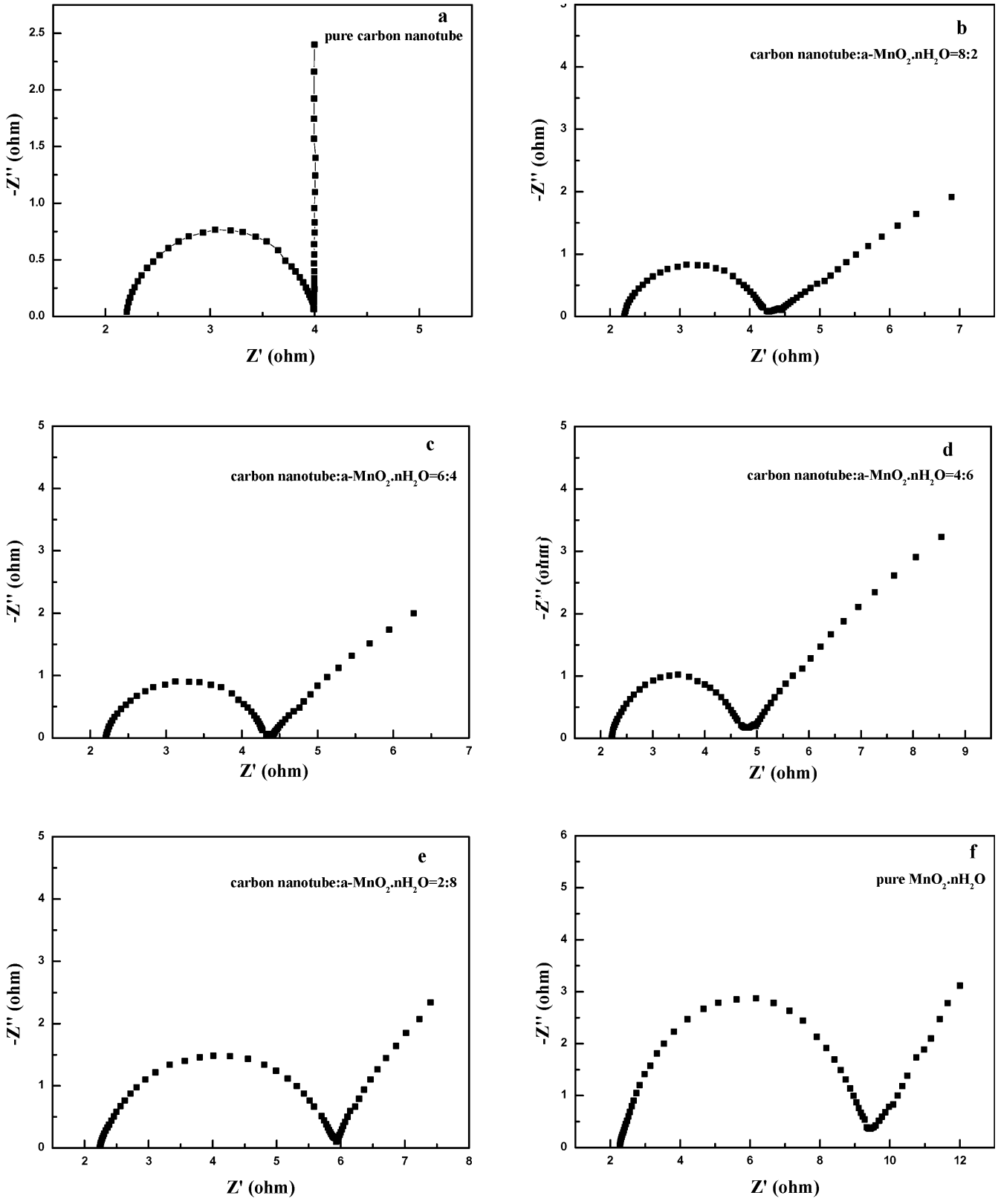

Fig. 6 Impedance Nyquist plots for different electrodes. Curves *a–f* represent pure carbon nanotubes, 8:2, 6:4, 4:6 and 2:8 composite electrodes and pure α-$MnO_2{\cdot}nH_2O$, respectively

At low frequencies, the impedance plot should theoretically be a vertical line, which is parallel to the imaginary axis. The carbon nanotubes show almost ideal capacitive behavior; however, the others show some

departure from that expected, which can also be explained by the electrode surface inhomogeneity and a "constant phase element" occurs [15], which results in the straight-line behavior of the Nyquist impedance with a slope angle smaller than $\pi/2$ for these electrodes, with the exception of the pure carbon nanotubes. This means that the porous electrodes have different pores with different dimensions and for the composite electrodes there exists some inhomogeneity in the surface, which leads to the low-frequency impedance behavior being shifted. Compared to the total impedance plots, we think that the d composite electrode has a smaller resistance and better capacitive behavior; it should be the most promising for use in electrochemical capacitors.

Conclusions

To achieve both high specific capacitance and high power simultaneously, adding a proper proportion of carbon nanotubes to hydrous manganese oxide to form a composite electrode may be an effective method. Comparing different ratios, the composite of 6:4 of α-$MnO_2{\cdot}nH_2O$ to carbon nanotubes was the most suitable for electrode materials in electrochemical capacitors. The reason may be due to the added carbon nanotubes lowering the electric resistivity and improving the contact between the α-$MnO_2{\cdot}nH_2O$ particles, and the surface of the α-$MnO_2{\cdot}nH_2O$ particles can work as an active site for rapid faradiac reactions.

References

1. Burke AF (1994) In: Nedell R (ed) Proceedings of the 36th power sources conference, Cherry Hill, NJ. IEEE, Piscataway, NJ, p 6
2. Miller JR (1995) In: Proceedings of the 5th international seminar on double layer capacitors and similar energy storage devices, Florida Educational Seminars Inc, Boca Raton, Fla, Dec 4–6
3. Isaacson MJ, Kraemer BJ, Laramore TJ, Mayer ST, Josephs LC (1996) Proceedings of the 37th power sources conference, Cherry Hill, NJ. IEEE, Piscataway, p 112
4. Jow TR, Zheng JP, Ding SP (1997) Proceedings of the 7th international seminar on double layer capacitors and similar energy storage devices, Florida Educational Seminars Inc, Deerfield Beach, Fla, Dec 8–10
5. Zheng JP (1999) Electrochem Solid-State Lett 2:359
6. Zheng JP, Jow TR (1995) J Electrochem Soc 142:L6
7. Zheng JP, Cygan PJ, Jow TR (1995) J Electrochem Soc 142:2699
8. Lee HY, Goodenough JB (1999) J Solid State Chem144:220
9. Lee HY, Kim SW, Lee HY (2001) Electrochem Solid State Lett 4:A19
10. Niu CM, Sichel EK, Hoch R, Moy D, Tennent H (1997) Appl Phys Lett 70:1480
11. Shan X, Dong GJ, Jing XY, Zhang ML (2001) Chin J Inorg Chem 17:669
12. Li XH, Zhang J, Li QW, Li HL, Liu ZF (2003) Carbon 41:598
13. Gamby J, Taberna PL, Simon P, Fauvarque JF, Chesneau M (2001) J Power Sources 101:109
14. Keiser H, Beccu K, Gutjahr MA, (1976) Electrochim Acta 21:539
15. Brug GJ, Van den Eeden ALG, Sluyters-Rehbach M, Sluyters JH (1984) J Electroanal Chem 176:275